Equation (A1) may now be expressed

$$E_d=a'\frac{\partial E_g}{\partial P}\left(\frac{a_{11}'}{Y_{11}}+\frac{a_\perp'}{Y_\perp}\right)^{-1}+a''\frac{\partial E_g}{\partial P}\left(\frac{a_{11}''}{Y_{11}}+\frac{a_\perp''}{Y_\perp}\right)^{-1} \quad \text{(A3)}$$

or

$$E_d=\frac{\partial E_g}{\partial P}Y_{11}Y_\perp\left(\frac{a'}{a_{11}'Y_\perp+a_\perp'Y_{11}}+\frac{a''}{a_{11}''Y_\perp+a_\perp''Y_{11}}\right). \quad \text{(A4)}$$

Using recent crystallographic data[35] and an experimentally determined value[36] of $\partial E_g/\partial P$ we obtain a value $E_d=11.1$ eV, which is in fair agreement with the figure of approximately 7 eV obtained from compressibility measurements[31] on trigonal Se. It is found that the contributions of the nearest and next-nearest neighbors to the deformation potential are approximately equal. This agrees with the estimate given by Treusch and Sandrock[2] and furthermore lends some justification to our initial assumption of considering the two components separately.

PHYSICAL REVIEW VOLUME 166, NUMBER 3 15 FEBRUARY 1968

Band Structure of Bismuth: Pseudopotential Approach*

STUART GOLIN†
Department of Mining, Metallurgy, and Petroleum Engineering, University of Illinois, Urbana, Illinois
and
Department of Physics, University of Pittsburgh, Pittsburgh, Pennsylvania

(Received 18 September 1967)

The electronic band structure of bismuth is studied by means of a pseudopotential approach. The Lin-Kleinman pseudopotential was adopted; its parameters were adjusted slightly to bring the band structure into agreement with two known energy differences in bismuth. With this pseudopotential, the band structure along symmetry lines and planes is calculated and the effective masses of the carriers are studied. The band structure is in good agreement with optical data and with effective-mass anisotropies, but the magnitude of the effective masses may differ from experiment by a factor of 3. Using the experimental effective masses and g factor of the holes, we infer the energy-level scheme at T near E_F. Also, we have tentatively identified a higher-lying band which has been experimentally observed. A very efficient method of calculating nonlocal and spin-orbit coupling terms in $\mathbf{k}\cdot\boldsymbol{\pi}$ perturbation theory is presented.

1. INTRODUCTION

THERE has been considerable interest in bismuth, both theoretical and experimental. Its interesting properties result largely from its carriers, which are very light and few in number. The Fermi surface is small and fairly simple, relaxation times are long, and quantum effects are relatively large. Because of these properties, bismuth has been used to develop many of the techniques used to study Fermi surfaces, and it makes a useful subject for other types of experiments, such as plasma studies.

Most theoretical studies have concentrated on the carriers themselves. Cohen and Blount[1] studied the g factor of the electrons, and Lax *et al.*[2] and Cohen[3] studied the dispersion of the electrons. Abrikosov and Falkovskii,[4] and Falkovskii and Razina[5] exploited the near-cubic symmetry of bismuth to study the small but important regions of the Brillouin zone near T and L where the carriers are located. Mase[6] made a more extensive tight-binding calculation which has correctly predicted the locations and symmetries of the carriers. However, his calculation is not sufficiently detailed to study properties such as optical reflectivity.

A detailed band-structure calculation is needed to study the effective masses[7] and g factors,[8] the optical properties,[9] Bi-Sb alloys,[10] and pressure effects.[11] A

* Research sponsored by the U. S. Air Force Office of Scientific Research, Office of Aerospace Research, U. S. Air Force, under Grant Nos. AF803 and AFOSR 196-66.

† Present address: Department of Physics, University of Pittsburgh, Pittsburgh, Pa. 15213.

[1] M. H. Cohen and E. I. Blount, Phil. Mag. **5**, 115 (1960).

[2] B. Lax, J. G. Mavroides, H. J. Zeiger, and R. J. Keyes, Phys. Rev. Letters **5**, 241 (1960); R. N. Brown, J. G. Mavroides, and B. Lax, Phys. Rev. **129**, 2055 (1963).

[3] M. H. Cohen, Phys. Rev. **121**, 387 (1961).

[4] A. A. Abrikosov and L. A. Falkovskii, Zh. Eksperim. i Teor. Fiz. **43**, 1089 (1962) [English transl.: Soviet Phys.—JETP **16**, 769 (1963)].

[5] L. A. Falkovskii and G. S. Razina, Zh. Eksperim. i Teor. Fiz. **49**, 265 (1965) [English transl.: Soviet Phys.—JETP **22**, 187 (1966)].

[6] S. Mase, J. Phys. Soc. Japan **13**, 434 (1958); **14**, 584 (1959).

[7] The various Fermi surface measurements are now in substantial agreement. For extensive bibliographies, see R. N. Bhargava, Phys. Rev. **156**, 785 (1967); W. S. Boyle and G. E. Smith, Progr. Semicond. **7**, 1 (1963); IBM J. Res. Develop. **8**, 215 (1964).

[8] G. E. Smith, G. A. Baraff, and J. M. Rowell, Phys. Rev. **135**, A1118 (1964). [Recent g-factor measurements are in good agreement with these results; B. McCombe and G. Seidel, Phys. Rev. **155**, 633 (1967)].

[9] M. Cardona and D. L. Greenway, Phys. Rev. **133**, A1685 (1964).

[10] See, e.g., J. J. Hall and S. H. Koenig, IBM J. Res. Develop. **8**, 241 (1964).

[11] See, e.g., A. L. Jain and R. Jaggi, Phys. Rev. **135**, A708 (1964).

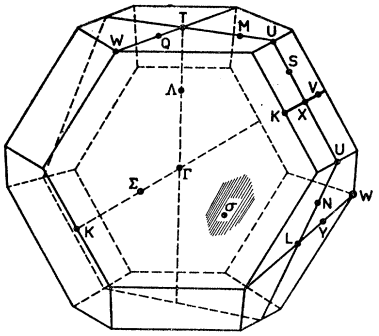

FIG. 1. The Brillouin zone for Bi, showing symmetry points, lines, and planes. For a more detailed description of the crystal and Brillouin zone structure, see Refs. 3 and 16.

first-principle calculation without any adjustable parameters simply can not be done with sufficient accuracy to give some of the important energy differences, which are of the order of 0.01 eV. Further, such a calculation is difficult because of the low symmetry of the bismuth crystal and because of the large atomic number, which necessitates the solution of the Dirac equation.[12,13]

Because of the wealth of experimental knowledge now available, a phenomenological study seemed feasible, and we chose the pseudopotential method.[14,15] Using only three adjustable parameters, we are able to account for the effective-mass anisotropies and for many other properties of bismuth.

The Brillouin zone of bismuth is shown in Fig. 1 with several symmetry points. We follow the general notation of Ref. 16, but contract the group-theoretical notation somewhat: L_5 and L_6 are degenerate under time reversal, so we write $L_s \equiv L_5+L_6$, as they are also symmetric under inversion. Similarly we write $L_a \equiv L_7+L_8$ for the degenerate antisymmetric levels. Similarly $X_s \equiv X_5+X_6$ and $X_a \equiv X_7+X_8$. At T, T_4^+ and T_5^+ are degenerate and we write $T_{45}^+ \equiv T_4^+ + T_5^+$, and similarly for T_{45}^- and $\Gamma_{45}^\pm$. The crystal-structure parameters are listed in Table I.

Atomic units (a.u.) will be used throughout: $e=\hbar=m_0=1$; the atomic unit of energy is 1 Hartree = 27.2 eV.

2. THE PSEUDOPOTENTIAL AND MOMENTUM-MATRIX ELEMENTS

A. The Pseudopotential

The pseudopotential method expresses the validity of the nearly-free-electron model: The energy bands are given by the free-electron kinetic energies modified by some weak pseudopotential. The real crystal potential which the valence electrons see is much larger than the pseudopotential, but Phillips and Kleinman[14] and others[15] have shown that both potentials have the same set of eigenvalues. The pseudo wave functions ψ_{nk}, similar to the real wave functions in the bulk of the crystal, are very much smoother than the real ones near the nuclei and can be conveniently expanded in plane waves. (The subscript n includes the spin index.) They satisfy the pseudopotential equation

$$[\tfrac{1}{2}p^2+V]\psi_{nk}=E_{nk}\psi_{nk}. \quad (1)$$

The pseudopotential V may be calculated from first principles, or one may choose a "reasonable" form with a few adjustable parameters. The parameters are then adjusted until the resulting band structure agrees with experiment. The latter has been the more popular approach, and the one we adopt.

Many different forms of V have been reported in the literature; we chose the form which was used successfully by Lin and Kleinman[17] (LK) to study the Pb salts. Their pseudopotential has the advantage of an intuitively reasonable form and few adjustable parameters. It consists of three distinct parts: $V_{\rm loc}$, a local potential which is the dominant term; V_s, an l-dependent term which increases the energies of the levels with s-atomic character; and $V_{\rm so}$, a term representing the spin-orbit coupling. (Our spin-orbit term is actually closer to Weisz's[18] form than that of LK.) These potentials are given by their matrix elements with plane waves:

$$V=V_{\rm loc}+V_s+V_{\rm so}, \quad (2)$$

$$\langle \mathbf{k}\alpha|V_{\rm loc}|\mathbf{k}'\alpha'\rangle = 4\pi Z\beta\Omega_0^{-1}G^{-2}(\beta^2+G^2)^{-1}S(\mathbf{G})\delta_{\alpha\alpha'} \times\{G\sin Gr_0-\beta\cos Gr_0\}, \quad (3)$$

$$\langle \mathbf{k}\alpha|V_s|\mathbf{k}'\alpha'\rangle = AB_{50k}B_{50k'}S(\mathbf{G})\delta_{\alpha\alpha'}, \quad (4)$$

$$\langle \mathbf{k}\alpha|V_{\rm so}|\mathbf{k}'\alpha'\rangle = -i\lambda f(k)f(k')S(\mathbf{G})\langle\alpha|\boldsymbol{\sigma}|\alpha'\rangle\cdot\mathbf{k}\times\mathbf{k}', \quad (5)$$

TABLE I. Crystal-structure parameters of bismuth at 4.2°K.[a]

Symbol[b]	Value (a.u.)	Definitions and remarks
$\lvert\mathbf{a}_i\rvert$	8.9247	Length of primitive translation vector
α	57°19′	Rhombohedral angle
u	0.23407	Internal displacement parameter
$\lvert\boldsymbol{\tau}\rvert$	5.2184	Half the minimum distance between atoms along trigonal direction
Ω_0	471.59	Volume of unit cell
$(2\pi)^3/\Omega_0$	0.52599	Volume of Brillouin zone
k_F	0.85628	Free-electron Fermi momentum
E_F	0.36661	Free-electron Fermi energy
a_0	6.3081	Lattice parameter[b]
g_0	0.50873	Lattice parameter[b]
ϵ	0.04046	Lattice parameter[b]

[a] These values were taken or calculated from C. S. Barrett [Australian J. Phys. 13, 209 (1960)], and P. Cucka and C. S. Barrett [Acta Cryst. 15, 865 (1962)].
[b] For a complete explanation of notation, see Appendix A of Ref. 16.

[12] P. Soven, Phys. Rev. **137**, A1706 (1965).
[13] T. L. Loucks, Phys. Rev. **139**, A1333 (1965).
[14] J. C. Phillips and L. Kleinman, Phys. Rev. **116**, 287 (1959).
[15] For an excellent discussion and bibliography of pseudopotentials, see W. A. Harrison, *Pseudopotentials in the Theory of Metals* (W. A. Benjamin, Inc., New York, 1966).
[16] L. M. Falicov and S. Golin, Phys. Rev. **137**, A871 (1965).
[17] P. J. Lin and L. Kleinman, Phys. Rev. **142**, 478 (1966).
[18] G. Weisz, Phys. Rev. **149**, 504 (1966).

where

$$\mathbf{G}=\mathbf{k}-\mathbf{k}', \tag{6}$$

$$S(\mathbf{G})=2\cos\mathbf{G}\cdot\boldsymbol{\tau}, \quad \text{(structure factor)} \tag{7}$$

$$f(k)=B_{51k}/k, \tag{8}$$

$$B_{nlk}=\int_0^\infty rj_l(kr)P_{nl}(r)\,dr. \tag{9}$$

Here α is the spin index and $\boldsymbol{\sigma}$ is the Pauli spin operator. The crystal-structure parameters Ω_0 and $\boldsymbol{\tau}$ are listed in Table I; and the pseudopotential parameters Z, β, r_0, A, and λ are listed in Table III. The orthogonalization coefficients B_{nlk} were calculated with Herman and Skillman's[19] atomic wave functions $P_{nl}(r)$, and approximated in analytic form:

$$B_{50k}\cong 1.125\exp(-bk^2), \tag{10}$$

$$b=0.332, \tag{10'}$$

$$f(\mathbf{k})=f(k)\cong\max\{0.7(1-0.36k),0\}. \tag{11}$$

It should be mentioned that the k dependence of $f(k)$ is appreciable for the values of k of interest here, although it is unimportant for tin.[18]

The pseudo wave functions were expanded into the equivalent of about 80 plane waves for each spin, or about 160 terms. Group theory was used to factor the secular equation as much as possible. For the points of highest symmetry, the machine time required to set up the secular equation far exceeded the diagonalization time. In this case, Luehrmann's "greater matrix element theorem"[20] was of considerable value, reducing the time required to evaluate a matrix element by as much as a factor of 12. The calculations were performed on the IBM 7090 computers at the University of Illinois and the University of Pittsburgh.

B. Matrix Elements of $\boldsymbol{\pi}$

In studying the effective masses of the carriers, the $\mathbf{k}\cdot\boldsymbol{\pi}$ perturbation theory[21] proved very useful, especially for the electrons where the two-band model is appropriate. Further, the matrix elements of $\boldsymbol{\pi}$ are needed to calculate g factors.[1] Corresponding to the three terms in the pseudopotential, Eq. (2), there are three terms in $\boldsymbol{\pi}$:

$$\boldsymbol{\pi}=\mathbf{p}+\boldsymbol{\pi}_s+\boldsymbol{\pi}_{so}, \tag{12}$$

$$\langle\mathbf{k}\alpha|\,\mathbf{p}\,|\mathbf{k}'\alpha'\rangle=\mathbf{k}\delta_{\alpha\alpha'}\delta_{\mathbf{k}\mathbf{k}'}, \tag{13}$$

$$\langle\mathbf{k}\alpha|\,\boldsymbol{\pi}_s\,|\mathbf{k}'\alpha'\rangle=A\delta_{\alpha\alpha'}S(\mathbf{G})(\nabla_{\mathbf{k}}+\nabla_{\mathbf{k}'})[B_{50k}B_{50k'}], \tag{14}$$

$$\langle\mathbf{k}\alpha|\,\boldsymbol{\pi}_{so}\,|\mathbf{k}'\alpha'\rangle=i\lambda f(k)f(k')S(\mathbf{G})\langle\alpha|\,\boldsymbol{\sigma}\,|\alpha'\rangle\times\mathbf{G}, \tag{15}$$

where $\mathbf{G}=\mathbf{k}-\mathbf{k}'$. Equations (14) and (15) are derived in Appendix A. The first term $\mathbf{p}$ is the dominant one and also the easiest one to calculate. The other two terms are usually neglected, but in bismuth each may be $\sim$20% of the total. The problem in evaluating these latter terms is simply that there are very many of them because the off-diagonal ones do not vanish. Treated in a straightforward way, they require an exorbitant amount of machine time to evaluate. However, with a simple trick, they may be evaluated as quickly as the first term. This is explained in Appendix B.

TABLE II. Some momentum-matrix elements.[a]

	$j=2$	$j=3$	$j=4$
$\pi_j^{(2)}$	$0.088+0.187i$	$-0.189+0.100i$	
$\pi_{j3}^{(3)}$	-0.103	-0.128	
$\pi_{3j}^{(3)}$	0.102	-0.128	
$\pi_{j3}^{(4)}$	-0.208	0.175	
$\pi_{3j}^{(4)}$	0.196	0.175	
$\pi_{j3}^{(5)}$	$-0.192+0.229i$	$0.276-0.086i$	$-0.078-0.079i$
$\pi_{3j}^{(5)}$	$-0.104-0.196i$	$0.276-0.086i$	$0.137-0.241i$
$\pi_{j3}^{(6)}$	$0.002+0.028i$	$-0.039+0.049i$	$-0.057+0.177i$
$\pi_{3j}^{(6)}$	$-0.108-0.034i$	$-0.039+0.049i$	$0.030+0.046i$
$\pi_{j3}^{(7)}$	$-0.065+0.217i$	$0.050+0.235i$	$-0.118+0.070i$
$\pi_{3j}^{(7)}$	$-0.075-0.051i$	$0.050+0.235i$	$-0.236-0.030i$
$\pi^{(1)}=0.168$			

[a] Refers to Eq. (16). Calculated using the "final" pseudopotential in Table III.

When all three terms are included in $\boldsymbol{\pi}$, the $\mathbf{k}\cdot\boldsymbol{\pi}$ method gives, in the two-band model, electron masses within 2% of the masses determined directly by calculating E as a function of $\mathbf{k}$. (The error is larger in the heavy-mass direction where the other bands are important.) The remaining discrepancy is partly due to the effect of other bands, and partly due to the omission of an additional contribution to $\boldsymbol{\pi}_{so}$, which reflects the dependence of f on k (see Appendix A).

We now list some matrix elements of $\boldsymbol{\pi}$ using the notation that $T_6^+(i)$ is the ith T_6^+ level, where each Kramers doublet, T_6^+ and UT_6^+, is counted once. Here U is related to the time-reversal operator.[1] The matrix elements expressed in the binary, bisectrix, trigonal coordinate system[22] take the form[23]

$$\begin{aligned}
&\langle T_4^-(1)|\,\boldsymbol{\pi}\,|UT_4^+(1)\rangle=\pi^{(1)}(0,0,1),\\
&\langle T_4^-(1)|\,\boldsymbol{\pi}\,|T_6^+(j)\rangle=\pi_j^{(2)}(-1,+i,0),\\
&\langle T_4^-(1)|\,\boldsymbol{\pi}\,|UT_6^+(j)\rangle=\pi_j^{(2)}(-1,-i,0),\\
&\langle T_6^+(j)|\,\boldsymbol{\pi}\,|T_6^-(j')\rangle=\pi_{jj'}^{(3)}(0,0,1),\\
&\langle T_6^+(j)|\,\boldsymbol{\pi}\,|UT_6^-(j')\rangle=\pi_{jj'}^{(4)}(-1,+i,0),\\
&\langle L_5(j)|\,\boldsymbol{\pi}\,|L_7(j')\rangle=\pi_{jj'}^{(5)}(1,0,0),\\
&\langle L_6(j)|\,\boldsymbol{\pi}\,|L_7(j')\rangle=(0,-\pi_{jj'}^{(6)},\pi_{jj'}^{(7)}).
\end{aligned} \tag{16}$$

The values of some of these parameters are listed in Table II.

[19] F. Herman and S. Skillman, *Atomic Structure Calculations* (Prentice-Hall, Inc., Englewood Cliffs, N. J., 1963).
[20] A. W. Luehrmann, Advan. Phys. (to be published).
[21] See e.g., C. Kittel, *Quantum Theory of Solids* (John Wiley & Sons, Inc., New York, 1963), pp. 179 ff.
[22] To specify the binary, bisectrix, and trigonal axes uniquely, we follow the convention of M. Cardona and D. L. Greenway, Phys. Rev. **133**, A1685 (1964).
[23] The exact form of the matrix elements may depend on the irreducible representations used; i.e., any linear combination of T_6^+ and UT_6^+ could be called T_6^+.

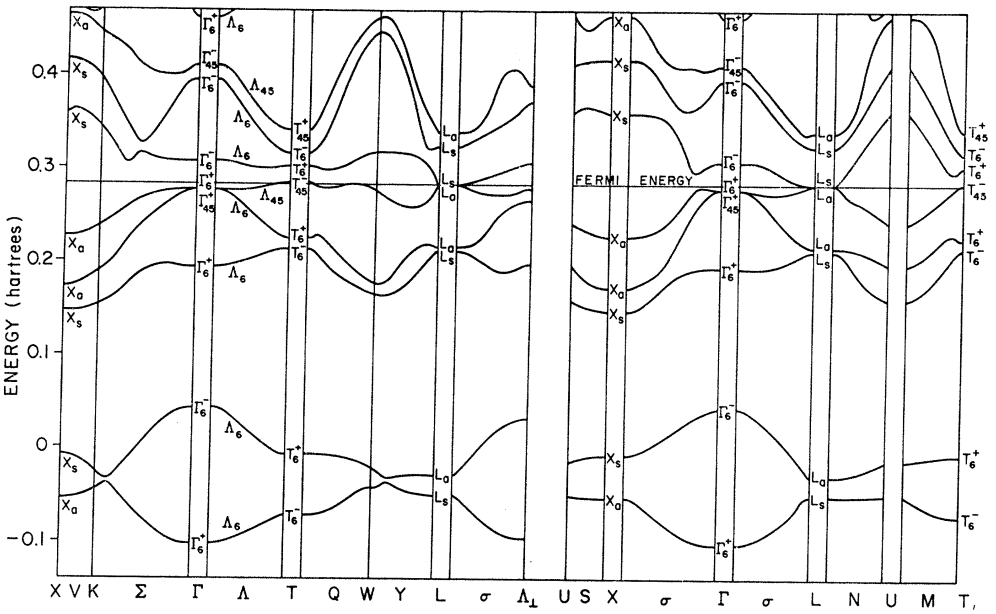

FIG. 2. The band structure of bismuth along various lines and planes. [The direction L-$\Lambda_\perp$ is perpendicular to the trigonal axis ($\Lambda_\perp$ is on that axis) and is of interest in interpreting tunneling measurements. See C. B. Duke (private communication); see also D. J. Ben-Daniel and C. B. Duke, Phys. Rev. Letters 14, 902 (1965).]

3. RESULTS OF CALCULATION AND COMPARISON WITH EXPERIMENT

We estimated the pseudopotential parameters following the procedures and results of Ref. 17. These parameters yield a plausible over-all band structure for bismuth, but there are three discrepancies in detail: The energy gap at L is too large, the overlap of the fifth and sixth bands (the sum of the electron and hole Fermi energies) is incorrect, and there are carriers at Γ. The adjustment of three of the parameters, Z, A, and λ, removed these discrepancies. The experimental values of the energy gap and overlap to which the pseudopotential was fit are[8]

$$E_g = E[L_s(3)] - E[L_a(3)] = 0.000564 \text{ a.u.},$$
$$E_0 = E[T_{45}^-(1)] - E[L_s(3)] = 0.00142 \text{ a.u.} \quad (17)$$

The initial and final pseudopotential parameters are given in Table III.

It should be pointed out that the choice of T as the site of the holes is somewhat arbitrary. This is the site found by Mase,[6] but we are unaware of any convincing evidence which rules out Γ, which has the same symmetry as T, as a possible site. The pseudopotential is not decisive either, but it would be more difficult to get comparable agreement with experiment at Γ, e.g., in the effective masses. Similarly one could try to put the electrons at X rather than at L, but this would require a drastic change in the pseudopotential to approximate the known effective masses. (Jain and Koenig[24] definitely established that the holes are at T or Γ, and that the electrons are at X or L.)

Note added in proof. Recent phonon and electron-hole recombination studies [S. H. Koenig, A. A. Lopez, D. B. Smith, and J. L. Yarnell, Phys. Rev. Letters **20**, 48 (1968)] show that either the electrons are at L and the holes at T, or that the electrons are at X and the holes at Γ. The former is most probably the case.

It should also be mentioned that the quantitative discrepancies in the effective masses described below could obviously be reduced by varying more param-

TABLE III. Pseudopotential parameters.[a]

	r_0	β	Z	λ	A
Initial values	0.474[b]	3.37[b]	3.3[c]	0.0147[c,d]	0.017[c,d]
Final values	0.474	3.37	3.013	0.0125	0.00993

[a] The matrix element in Eq. (3) is set to zero when $\mathbf{k}=\mathbf{k}'$ to avoid the infinity there. This defines the zero of energy.
[b] Calculated following the procedures of Ref. 17.
[c] Estimated from the values for lead from Ref. 17.
[d] The wave functions from Ref. 19 were used.

TABLE IV. Energy levels at the symmetry points. (All energies below 5.5 a.u.)

T_6^-	−0.07297	Γ_6^+	−0.10304	L_s	−0.05181	X_a	−0.05404
T_6^+	−0.00770	Γ_6^-	0.04211	L_a	−0.03063	X_s	−0.00794
T_6^-	0.21348	Γ_6^+	0.19319	L_s	0.21124	X_s	0.14706
T_6^+	0.22511	Γ_{45}^+	0.27660	L_a	0.21527	X_a	0.17250
T_{45}^-	0.28382	Γ_6^+	0.27675	L_a	0.28183	X_a	0.22695
T_6^+	0.30238	Γ_6^-	0.30696	L_s	0.28240	X_s	0.35920
T_6^-	0.31572	Γ_6^-	0.39409	L_s	0.32348	X_s	0.41658
T_{45}^+	0.34081	Γ_{45}^-	0.40983	L_a	0.33867	X_a	0.46384
T_6^-	0.54653	Γ_6^+	0.46166			X_s	0.48064
		Γ_6^-	0.50635				
		Γ_{45}^-	0.51079				
		Γ_6^-	0.51860				

[24] A. L. Jain and S. H. Koenig, Phys. Rev. **127**, 442 (1962).

TABLE V. Comparison of effective masses[a] and g factor with experiment.

	Theory	Experiment[b]
	Holes	
$\beta\|\|$trigonal axis	0.4	1.45
$\beta\perp$trigonal axis	6.0	15.6
Δ_s/Δ_0: $\mathbf{H}\|\|$trigonal axis[c]	1.9	1.9
$\mathbf{H}\perp$trigonal axis[c]	0	<0.003
	Electrons	
β_1 (binary)	292	886
β_2	8.1	3.8
β_3	208	339
θ_τ[d]	$+10°$	$-6°$ [e]

[a] These are the reciprocal quadratic masses ($E=\frac{1}{2}\sum_i \beta_i k_i^2$) in the principal directions. The electron masses are those at the bottom of the band.
[b] Reference 8 (except θ_τ). There is substantial agreement in the current literature with these values.
[c] Ratio of spin to orbital splitting for $\mathbf{H}$ in the direction indicated. (The g factor is given by $g=\Delta_s/\mu_0 H$, where μ_0 is the Bohr magneton.)
[d] The tilt angle is the smallest of the two angles between the trigonal axis and the two principal axes of the electron "ellipsoid" in the mirror plane. The sign convention is that of L. M. Falicov and P. J. Lin, Phys. Rev. 141, 562 (1966).
[e] Most authors find this value $\pm 1°$ (see, e.g., Bhargava, Ref. 7); Ref. 8 finds 4.3°.

eters. We tried varying all five parameters in the LK pseudopotential and even varying each Fourier coefficient of the pseudopotential separately. However, we judged the resulting improvement in the agreement with experiment to be insufficient to justify varying so many parameters.

The over-all band structure along various symmetry lines and planes is drawn in Fig. 2. It is seen that there are many levels near the Fermi energy, which is consistent with the tunneling measurements of Esaki and Stiles.[25] The energy levels at the symmetry points are listed in Table IV.

A. Holes

The holes are at T, and are in a T_{45}^- level as suggested by Mase[6] and by the g-factor measurements of Smith, Baraff, and Rowell.[8] The quadratic masses and g factor of this level are in qualitative but not quantitative agreement with experiment, as seen in Table V. The discrepancies are due to errors either in the momentum-matrix elements or in the energy differences to nearby energy levels, or both. But as the matrix elements at T are less sensitive to changes in the pseudopotential than are the small energy differences, they are probably more reliable. In fact we can combine these matrix elements (Table II) with the experimental masses and g factors to determine the positions of the energy levels at T near E_F which have nonvanishing momentum matrix elements with T_{45}^-. These energies, relative to T_{45}^-, are listed in Table VI and are probably accurate to a factor of 2; the uncertainty is mainly that of the matrix elements and many-body effects (other bands may have some effect).

Note added in proof. J. J. Hauser and L. R. Testardi [Phys. Rev. Letters 20, 12 (1968)] have made tunneling measurements with Bi films and have found four conductance peaks at -0.027, -0.0037, $+0.0073$, and $+0.029$ a.u. While it is not clear how to interpret such measurements, three of these peaks occur at energies close to the "experimental" band gaps at T in Table VI. (The tunneling was parallel to the trigonal axis.)

[25] L. Esaki and P. J. Stiles, Phys. Rev. Letters 14, 902 (1965).

TABLE VI. The energy-band scheme at T near E_F.[a]

	$T_{45}^+(1)-T_{45}^-(1)$	$T_6^+(3)-T_{45}^-(1)$	$T_{45}^-(1)-T_6^+(2)$
Pseudopotential[b]	0.057	0.0186	0.070
Experimental[c]	0.028	0.0076	0.023

[a] Notation: $T_6^+(3)$ is the energy of the third T_6^+ level, etc. (Atomic units are used.)
[b] That is, from the "final" pseudopotential in Table III.
[c] Inferred from the momentum-matrix elements and the experimental masses and g factor (see text).

B. Electrons

There are only two types of symmetry levels at L (L_s and L_a) and we want to determine which of the two is the symmetry of the conduction band. The most direct measure of this symmetry comes from recent studies of electron-phonon recombination[26] which imply[27] that the electrons and holes have opposite symmetries with respect to inversion. Thus if the assignment of the holes to the T_{45}^- level is correct, then we can conclude that the electrons are in an L_s level. (Our "final" pseudopotential was chosen to put them there.)

The electron masses are compared with experiment in Table V. The agreement is qualitative, the large anisotropy is present, but there are magnitude errors of a factor of 2 or 3. Further, the tilt angle is off by 16°. [*Note added in proof.* R. D. Brown, R. L. Hartman, and S. H. Koenig (to be published) have just carefully remeasured the tilt angle and find $+6°$. This change in sign reduces our discrepancy to only 4°.]

There is considerable controversy over the dispersion law obeyed by the electrons. The two principal models, the Lax "two-band model"[2] and the Cohen model,[3] both agree that the law is

$$E(1+E/E_g)=\tfrac{1}{2}\beta(\hat{k})k^2, \tag{18}$$

when

$$\beta(\hat{k})\gg 1. \tag{19}$$

Equation (19) holds for most directions, but in the heavy-mass direction $\beta\sim 1$. The Lax model assumes Eq. (18) still holds, while Cohen modifies it with the inclusion of other bands. (In fact, even if there were no other bands, there are still terms of order k^2 which become important.) The Cohen model also neglects possibly important terms.[28]

[26] A. A. Lopez and S. H. Koenig, Solid State Commun. 4, 513 (1966).
[27] S. H. Koenig (private communication).
[28] J. O. Dimmock, MIT Lincoln Laboratory Reports Nos. 1, 41, 1964 (unpublished).

TABLE VII. Comparison of theoretical and experimental optical-band gaps.

Designation[a]	Location in Brillouin zone: Rectangular coordinate[b]	Trigonal coordinate[c]	Bands	Symbol	Energy (a.u.): Theory	Experiment[a]
E_2	(0.59, −0.43, 0.08)	[−0.116, 0.334, 0.084]	$5\rightarrow 6$	(no symmetry)	0.05	0.062
			$4\rightarrow 6$		0.09	
E_4	(1, −0.02, −0.02)	[0, 0.5, 0.5]	$5\rightarrow 6$	$X_a\rightarrow X_s$	0.13	0.18
	(1, −0.02, −0.02)	[0, 0.5, 0.5]	$4\rightarrow 6$	$X_a\rightarrow X_s$	0.19	
	(0.92, −0.10, 0.06)	[0, 0.5, 0.42]	$4\rightarrow 6$	A^b (near X)	0.19	
	(1.0, −0.19, 0.15)	[0, 0.584, 0.416]	$4\rightarrow 6$	B^b (near K)	0.19	
E_5	(0.24, 0.24, 0.24)	[0.25, 0.25, 0.25]	$4\rightarrow 9$[d]	$\Lambda_6\rightarrow\Lambda_6$	0.24	0.26

[a] See Ref. 9.
[b] See Ref. 31, especially Table I.
[c] See Ref. 16.
[d] In Sb, this is a $5\rightarrow 9$ transition between two bands of Λ_1 symmetry (Ref. 31) of the single group. When spin-orbit coupling is added, $\Lambda_1\rightarrow\Lambda_6$. This implies a $4\rightarrow 9$ transition in Bi because the fifth Λ level has symmetry Λ_{45}.

Experimentally it is difficult to distinguish between the Cohen[29] and Lax models because the condition that they be the same, Eq. (19), holds over most of the Fermi surface. Further, it is difficult to make measurements in the region in which they differ simply because of the relatively large effective mass there. Thus it is not surprising that some experiments find nonellipsoidal effects,[30] i.e., the Cohen model, while others (e.g., Bhargava, Ref. 7) favor the Lax model.

A sensitive test of the models is the change of anisotropy of the Fermi surface with E_F; the Lax model predicts no change. The easiest way to vary E_F is by doping (see, e.g., Bhargava, Ref. 7) but this has the disadvantage of making the heavy-mass direction even less accessible, because of impurity scattering. One should, however, be able to vary (reduce) E_F without increasing scattering by applying hydrostatic pressure. This should unambiguously determine the dispersion in the heavy-mass direction.

C. Optical Band Gaps

Cardona and Greenaway[9] have measured the reflectivity of As, Sb, and Bi, and found their spectra to be very similar. Lin and Phillips[31] then analyzed the spectrum of Sb with the pseudopotential method and were able to determine the locations in the Brillouin zone of the critical points responsible for three of the experimentally observed peaks. Because of the similarity of the Bi and Sb spectra, we assume that their critical points have approximately the same locations in their respective Brillouin zones. We have calculated the energy gaps at these points[32] and compare them with experiment in Table VII. The agreement is seen to be very good. (While Lin and Phillips list up to four transitions corresponding to a single peak, not all of them seem relevant in bismuth.)

The locations of the critical points responsible for the other optical peaks in Sb have not yet been determined. As symmetry points are critical points for optical transitions, it is tempting to compare the band gaps there with the remaining unidentified peaks. This comparison is made in Table VIII and is very suggestive. This must, however, be interpreted cautiously because the low joint density of states associated with many of the energy levels near E_F at symmetry points in the semimetals would tend to make their contributions to the optical spectrum small.[31]

TABLE VIII. Possible critical points of optical transitions.

Designation[a]	Energy[a] (a.u.)	Bands	Symbol	Energy (a.u.)
E_1	0.044	$5\rightarrow 7$	$L_a\rightarrow L_s$	0.042
E_3	0.11	$4\rightarrow 8$	$T_6^+\rightarrow T_{45}^+$[b]	0.12
		$4\rightarrow 7$	$L_a\rightarrow L_s$	0.11
E_6	0.32	$3\rightarrow 8$	$X_s\rightarrow X_a$	0.32

[a] See Ref. 9.
[b] Because the measurements (Ref. a above) were made with the electric field polarized perpendicular to the trigonal axis, $4\rightarrow 8$ transitions *exactly* at T are forbidden by symmetry.

D. Other Bands

Recent experiments[25,33] have found several band extrema near E_F, making it desirable for us to study some of the extrema in our band structure. But because of the expense of calculating energies at points of little or no symmetry, the wave functions were expanded into a small set of plane waves, about half that used for the symmetry points. In some cases, this can considerably distort the bands. With this note of caution, we list six band extrema in Table IX. Note that some of the apparent extrema in Fig. 2 are not absolute extrema. Thus if one searches for absolute minima starting from the "minima" along ΓX and along TU, one finds the same absolute minimum $\min_2$.

[29] It should be pointed out that comparisons of the Cohen model with experiment usually mistakingly assume that $m_2=m_2'$, i.e., that the conduction band and the valence band just below it are "mirror bands" in the heavy-mass direction as they are in light-mass directions. In fact, it has recently found [R. T. Bate and W. R. Hardin, Bull. Am. Phys. Soc. **12**, 286 (1967)] that $m_2'\ll m_2$.

[30] V. S. Edelman and M. S. Khaikin, Zh. Eksperim i Teor. Fiz. **49**, 107 (1965) [English transl.: Soviet Phys.—JETP **22**, 77 (1966)].

[31] P. J. Lin and J. C. Phillips, Phys. Rev. **147**, 469 (1966).

[32] While the actual critical points in Bi may be displaced somewhat from these, the energy gaps will be the same to first order in the displacement.

TABLE IX. Band extrema[a] near E_F.

Label	Degeneracy	Approximate position in Brillouin zone[b]	Reciprocal effective masses[c] β_{11}	β_{12}	β_{13}	β_{22}	β_{23}	β_{33}	Description[d]
$\min_1$	6	[0.5, 0.58, 0.42]	0.9	0	0	19	−4	1.6	minimum on $\Sigma(TW)$
$\min_2$	12	[0.41, 0.54, 0.47]	13	−6.2	−2.9	4.2	+1.4	1.2	general point
$\min_3$	2	[0.33, 0.33, 0.33]	3.3	0	0	3.3	0	0.56	minimum of Λ_6
$\max_1$	6	[0.05, 0.15, 0.15]	0.8	0	0	4	−2	2	maximum in σ
$\max_2$	6	[0.5, 0.68, 0.32]	0.5	0	0	12	−2.5	2.5	maximum on $\Sigma(TW)$
$\max_3$[e]	12	[0.07, 0.14, −0.06]	1.4	0	0	1.5	+1.1	2.7	near maximum[e] on $\Sigma(\Gamma K)$

[a] These are maxima in the fifth band and minima in the sixth band. The energy differences between these extrema and E_F cannot be calculated reliably.
[b] In trigonal coordinates. See Ref. 16.
[c] $E=\frac{1}{2}\Sigma\beta_{ij}k_ik_j$ where k_i is measured from the extrema, and $\beta_{ij}=\beta_{ji}$. The coordinate system is defined by the binary, bisectrix, and trigonal axes (see Ref. 22).
[d] Σ is a binary axis parallel to the x direction; σ is a mirror plane perpendicular to the x direction.
[e] The maximum along $\Sigma(\Gamma K)$ disappears when a large expansion set is used. It may, however, reappear with a somewhat different pseudopotential.

Two levels were studied by de Haas–van Alphen-type measurements on doped samples.[33] Their minima are 0.0020 and 0.0026 a.u. above the bottom of the conduction band and have reciprocal cyclotron masses of 16 and 7, respectively, when the magnetic field is parallel to the trigonal axis. While the de Haas-van Alphen areas were observed to be constant as the magnetic field was rotated 20° from the trigonal axis, one can not conclude that the Fermi surfaces are nearly spherical. The hole ellipsoid, for instance, has an anisotropy in the quadratic masses of 10 and in the radii of 3, but it shows only a 4% variation in the de Haas–Van Alphen areas for this variation of the magnetic field.

None of the bands calculated in Table IX has a reciprocal cyclotron mass comparable to that of the lower-lying level. The $T_6^+(3)$ level could have a comparable mass if it were closer to T_{45}^- as indicated in Table VI. It is unlikely, however, that this is the observed level, for it would still lie much more than 0.0020 a.u. above $L_s(3)$ as observed experimentally.

We can, however, tentatively identify the higher-lying band with $\min_3$. The theoretical reciprocal mass is a factor of 2 too small, but this discrepancy would be largely reduced or eliminated if T_6^+ were lowered as suggested in Table VI. This identification could be checked experimentally by measuring the anisotropy of electrons in this band and by determining the number of equivalent minima, which is 2 for $\min_3$. (Because of the relatively high symmetry of $\min_3$, its masses were calculated using an equivalent secular equation as large as at T.)

4. SUMMARY AND CONCLUSIONS

By adjusting three parameters in the LK pseudopotential[17] to obtain two well-established energy differences in the band structure, we have calculated the band structure in much of the Brillouin zone. We have obtained good qualitative agreement with the effective masses and good quantitative agreement with the optical data. By combining effective-mass and g-factor measurements with momentum-matrix elements, we have proposed an energy-level scheme at T near E_F. Further, we have studied some band extrema near E_F and have tentatively identified one of them with a higher-lying level observed experimentally.

We have been unable to get quantitative agreement with the experimental effective masses, even when many parameters were varied. The difficulty may be due to a poor choice of pseudopotential or its parameters, or to many-body effects,[34] or it may represent a limitation of the pseudopotential method itself. Kleinman and Phillips[35] have found that in Si the core part of the orthogonalized plane wave contributes ~10% to the momentum-matrix elements. This effect should be larger in bismuth, which has a larger core.

It would not have been difficult to fit all of the effective masses to experiment using an enhancement factor of about 2, which would approximately double the theoretical-reciprocal effective masses. However, one would expect many-body effects[34] to have the opposite effect of halving the reciprocal masses, as seems to be the case in antimony.[36]

Because of many-body effects, it is undesirable to adjust a pseudopotential to fit effective masses. The fitting could be done much more precisely if several band gaps were known, making electroreflectance[37] or piezoreflectance[38] measurements highly desirable.

Finally we have shown how $\pi\cdot\mathbf{p}$ matrix elements may be calculated efficiently.

ACKNOWLEDGMENTS

I am very grateful to L. M. Falicov for several enlightening conversations and for a careful reading of the final manuscript. I wish to express my gratitude to Morrel H. Cohen for many illuminating discussions.

[33] G. A. Antcliffe and R. T. Bate, Phys. Letters **23**, 622 (1966).

[34] N. W. Ashcroft and J. W. Wilkins, Phys. Letters **14**, 285 (1965).

[35] L. Kleinman and J. C. Phillips, Phys. Rev. **118**, 1153 (1960).

[36] W. R. Datars and J. Vanderkooy, J. Phys. Soc. Japan Suppl. **21**, 657 (1966).

[37] B. O. Seraphin and R. B. Hess, Phys. Rev. Letters **14**, 138 (1965).

[38] W. E. Engeler, H. Fritzsche, M. Garfinkel, and J. J. Tiemann, Phys. Rev. Letters **14**, 1069 (1965).

Also, I want to thank Gideon Weisz, S. H. Koenig, P. J. Lin, G. E. Smith, and J. C. Phillips for useful conversations.

APPENDIX A

The purpose of this Appendix is to derive Eqs. (14) and (15) which generalize $\mathbf{k}\cdot\boldsymbol{\pi}$ perturbation theory to our Hamiltonian. The derivation parallels the standard procedure.[21]

The Hamiltonian is

$$H=\tfrac{1}{2}p^2+V_{\rm loc}+V_s+V_{\rm so}\,, \tag{A1}$$

where the potentials are defined in Eqs. (3)–(9). $V_{\rm so}$ is often put in the form[21]

$$V_{\rm so}=(1/4c^2)\boldsymbol{\sigma}\times\nabla W\cdot\mathbf{p}\,, \tag{A2}$$

where W is a superposition of atomic potentials. We assume W to be local. To relate W to our $V_{\rm so}$, we calculate the matrix elements between plane waves of $V_{\rm so}$ as defined in Eq. (A2) and compare it with Eq. (5).

From Eq. (A2) we find

$$\langle\mathbf{q}\alpha|\,V_{\rm so}\,|\mathbf{q}'\alpha'\rangle=i(1/4c^2)S(\mathbf{G})W_G\langle\alpha|\boldsymbol{\sigma}|\alpha'\rangle\times\mathbf{q}\cdot\mathbf{q}'\,, \tag{A3}$$

where

$$\mathbf{G}=\mathbf{q}-\mathbf{q}' \tag{A4}$$

is a reciprocal lattice vector and where W_G is the Fourier transform of W. We have used the relation

$$\langle\mathbf{q}|\,\nabla W\,|\mathbf{q}'\rangle=i\mathbf{G}S(\mathbf{G})W_G\,, \tag{A5}$$

which we get by integrating by parts. Comparing Eqs. (A3) and (5) we see that

$$W_G=-4c^2\lambda f(q)f(q')\,. \tag{A6}$$

This equation makes sense only if $f(q)$ is independent of q, i.e., if W is local. (λ, however, may depend on $\mathbf{G}$.) While the dependence of f on q is in fact appreciable [Eq. (11)], ignoring that dependence here leads to errors of only $\sim 1\%$ in the effective masses.

In $\mathbf{k}\cdot\boldsymbol{\pi}$ perturbation theory, we are interested in the energy bands near a local extremum which we take to be $\mathbf{k}_0$. Let $\mathbf{k}$ be the distance from $\mathbf{k}_0$ to a nearby point $\mathbf{k}'$:

$$\mathbf{k}'=\mathbf{k}_0+\mathbf{k}\,. \tag{A7}$$

We now calculate $E_{n\mathbf{k}'}-E_{n\mathbf{k}_0}$ to second order in $\mathbf{k}$ using second-order perturbation theory.

From the Bloch theorem

$$\psi_{n\mathbf{k}'}=e^{i\mathbf{k}'\cdot\mathbf{r}}u_{n\mathbf{k}'}=e^{i\mathbf{k}\cdot\mathbf{r}}\phi\,, \tag{A8}$$

where $u_{n\mathbf{k}'}$ has the periodicity of the lattice and where

$$\phi\equiv e^{i\mathbf{k}_0\cdot\mathbf{r}}u_{n\mathbf{k}'} \tag{A9}$$

has the Bloch form for the point $\mathbf{k}_0$.

Then

$$\begin{aligned}0&=[H-E_{n\mathbf{k}'}]\psi_{n\mathbf{k}'}=[H-E_{n\mathbf{k}'}]e^{i\mathbf{k}\cdot\mathbf{r}}\phi\\&=e^{i\mathbf{k}\cdot\mathbf{r}}[\tfrac{1}{2}(\mathbf{p}+\mathbf{k})^2+V_{\rm loc}+V_s'\\&\qquad+(1/4c^2)\boldsymbol{\sigma}\times\nabla W\cdot(\mathbf{p}+\mathbf{k})-E_{n\mathbf{k}'}]\phi\,,\end{aligned} \tag{A10}$$

where

$$V_s'\equiv e^{-i\mathbf{k}\cdot\mathbf{r}}V_se^{i\mathbf{k}\cdot\mathbf{r}}\,. \tag{A11}$$

($V_s'=V_s$ when V_s is local.) The equation for ϕ can be written

$$[H_0+H'-E_{n\mathbf{k}'}]\phi=0\,, \tag{A12}$$

where

$$H_0=\tfrac{1}{2}p^2+V_{\rm loc}+V_s+(1/4c^2)\boldsymbol{\sigma}\times\nabla W\cdot\mathbf{p} \tag{A13}$$

is independent of $\mathbf{k}$, and where

$$H'=\tfrac{1}{2}k^2+\mathbf{k}\cdot\mathbf{p}+(V_s'-V_s)+(1/4c^2)\boldsymbol{\sigma}\times\nabla W\cdot\mathbf{k}\,. \tag{A14}$$

Since ϕ has the Bloch form for $\mathbf{k}_0$, it can be expanded in terms of the $\psi_{m\mathbf{k}_0}$. Then

$$E_{n\mathbf{k}'}-E_{n\mathbf{k}_0}=\tfrac{1}{2}k^2+\sum_{m\neq n}\frac{|\langle\psi_{n\mathbf{k}_0}|H'|\psi_{m\mathbf{k}_0}\rangle|^2}{E_{n\mathbf{k}_0}-E_{m\mathbf{k}_0}}\,. \tag{A15}$$

Terms linear in $\mathbf{k}$ vanish because of the extremum at $\mathbf{k}=0$.

As we expand the ψ's in plane waves, we are only interested in the matrix elements of H' between plane waves. Further, we only need these elements to first order in $\mathbf{k}$ to give $E_{n\mathbf{k}'}$ correct to second order in $\mathbf{k}$.

For the nonlocal term in H' we have

$$\begin{aligned}&\langle\mathbf{q}\alpha|\,V_s'-V_s\,|\mathbf{q}'\alpha'\rangle\\&\quad=\langle\mathbf{q}+\mathbf{k},\alpha|\,V_s\,|\mathbf{q}'+\mathbf{k},\alpha'\rangle-\langle\mathbf{q}\alpha|\,V_s\,|\mathbf{q}'\alpha'\rangle\\&\quad=AS(\mathbf{G})\delta_{\alpha\alpha'}\{B_{50|\mathbf{q}+\mathbf{k}|}B_{50|\mathbf{q}'+\mathbf{k}|}-B_{50q}B_{50q'}\}\\&\quad=AS(\mathbf{G})\delta_{\alpha\alpha'}\nabla_{\mathbf{k}}\{B_{50|\mathbf{q}+\mathbf{k}|}B_{50|\mathbf{q}'+\mathbf{k}|}\}_{\mathbf{k}=0}\cdot\mathbf{k}\\&\quad=AS(\mathbf{G})\delta_{\alpha\alpha'}\mathbf{k}\cdot(\nabla_{\mathbf{q}}+\nabla_{\mathbf{q}'})(B_{50q}B_{50q'})\,,\end{aligned} \tag{A16}$$

where we have used Eqs. (A11) and (4).

For the spin-orbit coupling term

$$\begin{aligned}&\langle\mathbf{q}\alpha|\,(1/4c^2)\boldsymbol{\sigma}\times\nabla W\cdot\mathbf{k}\,|\mathbf{q}'\alpha'\rangle\\&\quad=i(1/4c^2)S(\mathbf{G})W_G\langle\alpha|\boldsymbol{\sigma}|\alpha'\rangle\times\mathbf{G}\cdot\mathbf{k}\\&\quad=-i\lambda f(q)f(q')S(\mathbf{G})\langle\alpha|\boldsymbol{\sigma}|\alpha'\rangle\times\mathbf{G}\cdot\mathbf{k}\,,\end{aligned} \tag{A17}$$

using Eqs. (A5) and (A6).

Therefore we can put Eq. (A15) into the standard form of $\mathbf{k}\cdot\boldsymbol{\pi}$ perturbation theory by writing

$$H'=\mathbf{k}\cdot\boldsymbol{\pi}\,, \tag{A18}$$

where

$$\boldsymbol{\pi}=\mathbf{p}+\boldsymbol{\pi}_s+\boldsymbol{\pi}_{\rm so}\,. \tag{A19}$$

The matrix elements of $\boldsymbol{\pi}_s$ and $\boldsymbol{\pi}_{\rm so}$ are given by Eqs. (14) and (15), as can be seen from Eqs. (A14) and (A16)–(A19).

Strictly speaking, $V_s'-V_s$ contains terms quadratic in $\mathbf{k}$ [as one can see by expanding the exponentials in Eq. (A11)] which should be included in Eq. (A15) in first-order perturbation theory. But this contribution to

the reciprocal effective mass is of order $A=0.01$, and is negligible.

APPENDIX B

The purpose of this Appendix is to show how the contributions to the matrix elements of π from the spin-orbit coupling and the nonlocal s shift may be readily calculated in the pseudopotential formulation.

Consider first the spin-orbit interaction between the two states ψ_{nk} and ψ_{mk}, where

$$\psi_{nk}=\sum_i a_{ni}|\mathbf{k}-\mathbf{G}_i,\alpha_i\rangle, \tag{B1}$$

the sum being over all translation vectors in the reciprocal lattice and both spin directions. Then, from Eq. (15), the desired matrix element is

$$\langle\psi_{nk}|\pi_{so}|\psi_{mk}\rangle=-i\lambda\sum_{ij}a_{ni}^*a_{mj}f(\mathbf{k}-\mathbf{G}_i)f(\mathbf{k}-\mathbf{G}_j)\times S(\mathbf{G}_j-\mathbf{G}_i)\langle\alpha_i|\boldsymbol{\sigma}|\alpha_j\rangle\times(\mathbf{G}_j-\mathbf{G}_i). \tag{B2}$$

The evaluation of this sum is straightforward but requires a considerable amount of work because the sum is over two indices; typically 25 000 terms must be calculated. This sum, however, can be broken into sums and products of a few terms in which each term is a sum over a single index. The resulting savings are considerable.

This reduction is effected when each term in the sum, Eq. (B2), depends only on a single index. This is already the case for all of the terms except S and $\boldsymbol{\sigma}$, and the reduction of the former is trivial:

$$\begin{aligned}S(\mathbf{G}_j-\mathbf{G}_i)&=2\cos[(\mathbf{G}_j-\mathbf{G}_i)\cdot\boldsymbol{\tau}]\\&=2\cos(\mathbf{G}_j\cdot\boldsymbol{\tau})\cos(\mathbf{G}_i\cdot\boldsymbol{\tau})\\&\quad+2\sin(\mathbf{G}_j\cdot\boldsymbol{\tau})\sin(\mathbf{G}_i\cdot\boldsymbol{\tau}).\end{aligned} \tag{B3}$$

To decompose σ it is necessary to express the matrix elements of the Pauli operator explicitly in terms of α_i and α_j. In general, the matrix elements of $\boldsymbol{\sigma}$ are

$$\begin{aligned}&\langle\uparrow|\boldsymbol{\sigma}|\uparrow\rangle=-\langle\downarrow|\boldsymbol{\sigma}|\downarrow\rangle=(0,0,1),\\&\langle\downarrow|\boldsymbol{\sigma}|\uparrow\rangle=\langle\uparrow|\boldsymbol{\sigma}|\downarrow\rangle^*=(1,i,0).\end{aligned} \tag{B4}$$

(The parentheses refer, in general, to rectangular coordinates, and here they refer to the binary, bisectrix, and trigonal axes.) If we now denote the state $\uparrow$ by $\alpha=+1$, and the state $\downarrow$ by $\alpha=-1$, we can write

$$\langle\alpha_i|\boldsymbol{\sigma}|\alpha_j\rangle=\tfrac{1}{2}\{(1-\alpha_i\alpha_j)(1,0,0)+\alpha_i(0,-i,1)+\alpha_j(0,i,1)\}. \tag{B5}$$

It can be readily verified that this satisfies Eq. (B4).

If we now substitute Eqs. (B3) and (B5) into Eq. (B2), the reduction into sums over a single index becomes clear. For example, one of the terms is

$$-i\lambda\{\sum_i a_{ni}^*\alpha_i f(\mathbf{k}-\mathbf{G}_i)\cos\mathbf{G}_i\cdot\boldsymbol{\tau}\}(0,-i,1)\times\{\sum_j a_{mj}\mathbf{G}_j f(\mathbf{k}-\mathbf{G}_j)\cos\mathbf{G}_j\cdot\boldsymbol{\tau}\}. \tag{B6}$$

While there are 20 such terms to evaluate, they may be evaluated quickly, and many terms may vanish due to symmetry.

The treatment of the contribution from the nonlocal term, Eq. (14), is very similar and need not be repeated except to note that we can write

$$\delta_{\alpha,\alpha'}=\tfrac{1}{2}(1+\alpha\alpha'), \tag{B7}$$

and that the gradient in Eq. (14) takes on a very simple form in our treatment. Using Eq. (10) we find

$$(\nabla_{\mathbf{k}}+\nabla_{\mathbf{k}'})[B_{50k}B_{50k'}]=-2bB_{50k}B_{50k'}(\mathbf{k}+\mathbf{k}'). \tag{B8}$$

It should be clear that a sum over a single index depends only on the wave function of a single energy level. The matrix elements of $\pi-\mathbf{p}$ between two energy levels is then a sum of several terms, each term being a product of a function of one of the levels with a function of the other. This fact is useful if one wants the matrix elements of one level with several others. It is especially important if one would want to base an extended $\mathbf{k}\cdot\mathbf{p}$ calculation[39] on a completed pseudopotential calculation, for this requires the momentum-matrix elements between all pairs of levels at one point in the Brillouin zone.

[39] F. H. Pollak and M. Cardona, J. Phys. Chem. Solids 27, 423 (1966).